Biomass and Bioenergy 145 (2021) 105931

Contents lists available at ScienceDirect

Biomass and Bioenergy

journal homepage: www.elsevier.com/locate/biombioe

Research paper

Urban bio-waste as a flexible source of electricity in a fully renewable energy system

Lotta B. van Leeuwen [a,b], Hans J. Cappon [a,b], Karel J. Keesman [c,*]

[a] Environmental Technology, Wageningen University & Research, Wageningen, The Netherlands
[b] Department of Technology, Water and Environment, HZ University of Applied Sciences, Middelburg, The Netherlands
[c] Mathematical and Statistical Methods - Biometris, Wageningen University & Research, PO Box 16, 6700AA Wageningen, The Netherlands

ARTICLE INFO

Keywords:
Renewable urban energy system
Optimal renewable energy planning
Urban bio-waste gasification
Electricity curtailment minimization

ABSTRACT

This study proposes a curtailment-minimization model to investigate the potential of urban bio-waste to provide flexible electricity to a wind and solar powered Amsterdam. The transition to solar and wind as primary sources of renewable energy is hampered by their intermittent nature. Being controllable, biomass energy holds the potential of providing both renewable and flexible power. For the transformation from urban bio-waste to electricity, a coupled gasifier and solid oxide fuel cell (SOFC) unit was used. An islanded microgrid for the residential area of Amsterdam was investigated on the basis of an average year, both in terms of weather and electricity consumption. The study aims at finding the optimal sizing of each component to provide sustainable and secure electricity supply. Security of electricity supply was guaranteed by ensuring a net positive daily energy balance while minimizing the total surplus energy to be curtailed during the year. All organic municipal solid waste (MSW) available was used representing 39% of the yearly electricity demand of Amsterdam; PV panels (20%) and wind turbines (41%) covered the remaining share. To this end, optimal PV and wind capacities of 186 MW and 165 MW were estimated, representing respectively 16.9% and 94.0% of the total potential capacity of Amsterdam. In this study, the use of urban bio-waste is proven to bring flexibility to the energy system: using more biomass allows lower curtailment values.

1. Introduction

Reduction in anthropogenic CO_2 emissions is perceived as an important measure to mitigate climate change and keep the increase in global average temperature below 2 °C [1]. In the power sector, shifting from fossil fuels to renewable energy (RE) resources is projected to contribute largely to this decarbonization. In Europe, a binding target of 32% share of RE is fixed for the gross final energy consumption in 2030, [2]. Most renewable energy sources have the property of being intermittent, making their implementation in the power system challenging. To improve the integration of intermittent RE, novel forms of flexibility are needed. "Flexibility" is defined by Holttinen et al. [3] as "the ability of an energy system to accommodate the variability and uncertainty in the load-generation balance while maintaining satisfactory levels of performance at any time-scale".

Several complementary options have been identified which add flexibility in the energy system, thereby facilitating the integration of intermittent RE resources in the energy mix. Firstly, renewables have most potential close to the consumer: besides a reduction of transmission and distribution line losses, distributed RE support the local power grid and improve the system's stability [4,5]. Interconnecting multiple renewable energy technologies further enhances the flexibility and reliability of the system. The weakness of one is compensated by the strength of the other. Usually, wind turbines and solar photovoltaics are combined for electricity production. However, such a hybridization makes the system more complex [6]. Secondly, intermittency of RE sources can be alleviated by using an appropriate Energy Storage System (ESS), which guarantees the energy system to meet peak electrical load demands by providing a suitable time varying energy management [7]. Different types of storage systems exist, such as batteries, capacitors, or hydrogen conversion systems. A combination of storage components makes the ESS even more robust. Finally, flexibility can be brought into an energy system by stimulating consumers' behavior with respect to energy consumption, depending on the energy availability (demand-response) [8,9].

Although wind and solar are the fastest growing renewable energy sources with an almost infinite potential, they represent only a modest share of 17% of the total renewable energy generated in Europe. Most of Europe's renewable energy derives from biomass, with a 50%

* Corresponding author.
E-mail address: karel.keesman@wur.nl (K.J. Keesman).

https://doi.org/10.1016/j.biombioe.2020.105931
Received 1 July 2020; Received in revised form 4 December 2020; Accepted 6 December 2020
Available online 14 January 2021

Glossary

BGSOFC	Biomass Gasification Solid Oxide Fuel Cell
SOFC	Solid Oxide Fuel Cell
MSW	Municipal Solid Waste
PV	Photovoltaic (solar cells)
RE	Renewable Energy
ESS	Energy Storage System
UB	Upper Boundary (of an optimization problem)
LB	Lower Boundary (of an optimization problem
IC	Inequality Constraint (of an optimization problem)
E_{tot}	Total net energy over one year
E_{net}	Net energy demand
E_{gen}	Generated energy
E_{pv}	Energy from solar
E_{wind}	Energy from wind
E_{bio}	Energy from biomass
η	Efficiency of conversion
κ	Fraction of total renewable energy source potential

share of the renewable energy production [10]. In the Netherlands, biomass represents about 70% of the generated renewable energy and is expected to still represent 56% in 2030 [11]. Unlike wind and solar, the biomass resource can be physically stored and used on demand. In fact, proper storage can ensure year-round availability of biomass for energy conversion, despite the seasonal variability due to harvesting [12]. In essence, biomass is at the same time a (controllable) renewable energy source and a storage element. This makes biomass a valuable component in any fully renewable energy system [13–15]. Moreover, using urban bio-waste instead of biomass directly coming from primary production (crops and wood) will help improving the sustainability of renewable urban energy systems.

Knowledge gap

Most of renewable energy design studies have been conducted for a combination of PV panels and wind turbines, with batteries as source of flexibility [16–18]. Less attention has been paid to hybrid energy production systems including PV, wind and biomass. Besides, studies which include biomass as an energy source have mostly been performed for rural locations, as most biomass available for energy purposes is issued from agriculture. A consensus exists on avoiding first generation bioenergy in order to avoid the food versus fuel trade-off, paving the way for second generation bioenergy sources [19,20]. Many examples of rural (micro)grids can be found, where local crop residues are integrated as an energy source in a renewable energy system. For example, Balamurugan et al. propose a photovoltaic–wind–biomass generation system for rural areas of India, where a biomass gasifier runs on agricultural residues [21]. In their work, Garrido et al. proposed food processing waste as a source of biomass for energy production in remote locations. Taking Mozambique as their case-study, they showed how cashew nut-shell usage offers a competitive alternative to diesel generators [22]. However, biomass is also locally available from urbanized regions, in the form of municipal solid waste (MSW) streams, rich in organic matter and thus a potential source of bioenergy [20]. Linking the urban bio-waste availability with the local demand can help balancing the electricity system. In the Netherlands, an estimated 100 PJ of urban biomass is available for energy, equivalent to 3% of the country's total yearly energy use [23]. Besides bringing a renewable source of flexibility in an energy system, urban bio-waste can contribute to more effective urban waste management. Jiang et al. investigated the potential of biomass as back-up electricity source for Amsterdam in the next decades, given different climate and energy policy scenarios [24]. They compared the role of bio-electricity in a business-as-usual, emission capping and renewable energy scenario using a cost minimization model.

The objective of this paper is to investigate and demonstrate the potential of bio-waste as a flexible source of residential electricity in a PV–wind powered city, taking Amsterdam as an example. The framework used is an islanded energy system model, which can be applied to any city. It has been chosen to generate all renewable electricity within the boundaries of the municipality in order to highlight the feasibility of local, decentralized power production. Optimal timing in converting bio-waste to electricity can increase energy security, even when the inflexible solar and wind resources are unavailable. Energy security is viewed here from a technical perspective, where demand is being met and curtailment minimized. The outcomes of this study are intended to guide researchers, policy makers and energy companies in identifying the potential role bio-waste could play in the energy transition, mainly by providing inter-seasonal flexibility. This hypothetical case, using real historical data, is not meant for direct implementation but to highlight and quantify future possibilities. The outline of this paper is as follows. In Section 2, the energy system and the modeling problem are formulated. Section 3 presents the results, which are discussed in Section 4. Finally, Section 5 contains some concluding remarks.

2. Methodology

The proposed methodology to answer the main research question *"what is the potential of urban bio-waste as a flexible source of electricity in a fully renewable energy system?"* is composed of three main stages: (1) formulation of a renewable energy system model for Amsterdam (Section 2.1), (2) enumerative optimization and (3) active-set optimization (Section 2.2). The complete model structure, representing a simplified potential energy system, is illustrated in Fig. 1. Note that additional storage capacity can be integrated into this model, like hydrogen storage before the fuel cell and (fast-response) battery storage connected to the DC-bus.

2.1. Energy system model description

A renewable energy (RE) model was formulated with the aim to balance sustainable electricity generation and residential consumption in Amsterdam. The model represents a simplified potential energy system of the Dutch capital city in islanded mode, without connections to the surrounding electricity network. In other words, electrical self-sufficiency is being mimicked. It was chosen to omit conventional storage options (batteries, capacitors) at this stage of the study in order to focus on the role of biomass. Despite an initial temporal resolution of input data of one hour, the energy model was run for daily steps as this work concentrates on the inter-seasonal contribution of bio-waste in a RE mix. Energy technologies selected are: solar photovoltaics (PV), inland wind turbines and Biomass Gasification-Solid Oxide Fuel Cells (BGSOFC). The RE model is divided into four modules, respectively for calculating the production of solar, wind and bio-electricity, as well as the daily consumption of residential electricity.

2.1.1. Solar and wind modules

Sustainable electricity is produced by local RE sources available within the boundaries of the city. Both the solar and wind modules need weather data as input to generate electricity production. Open-source irradiation, temperature and windspeed data from the Dutch meteorological institute KNMI were used [25]. Average data from 1994 to 2014 were taken to represent a representative yearly pattern. Solar irradiation and temperature were fed into a photovoltaic thermal efficiency system model Appendix A while windspeeds were fed in a windturbine power curve system model Appendix B. Historical cloud cover and wind profiles were assumed to be still representative at the time of the study. Maximum capacities for solar and wind are

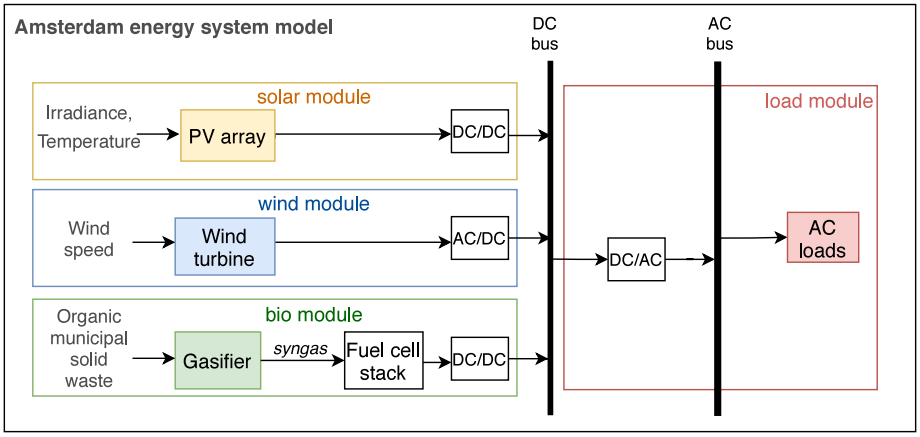

Fig. 1. Overview of the modeling framework for residential renewable electricity supply.

determined by space availability within the municipality of Amsterdam. The maximum potential PV capacity is limited by the total roof area suitable for solar panels, estimated at 7.7 km^2 (equivalent to 1100 MW, or approximately 1044 GWh electricity production) [26,27]. In 2019, the installed capacity of PV panels was 50 MW, or 4.5% of the total suitable roof area [27]. The maximum installed capacity for wind turbines in Amsterdam is estimated at 175 MW [26,27]. In 2019, the total installed capacity of wind turbines was 66 MW, or roughly 38% coverage of the total potential, responsible for a power production of 128 GWh that year [27].

2.1.2. Biomass module

Input for the biomass module was defined by the availability of urban bio-waste for electricity production in Amsterdam. In this study, the focus was on residential and industrial organic Municipal Solid Waste (MSW), considered to hold the largest energetic potential of all urban bio-waste streams with 1300 ton/d available [24]. This MSW is considered to be steadily available throughout the whole year and can act as a continuous energy storage buffer.

Biomass conversion to electricity can be realized by conventional fueled power plant technologies, offering consolidated technologies but low electrical efficiencies (20%). Higher efficiencies (40% elec) can be reached by coupling biomass gasification with electrochemical devices such as Solid Oxide Fuel Cells (SOFCs) [28]. Gasification is a feedstock flexible technology, able to handle heterogeneous bio-waste containing lignocellulosic material [29]. In the past decade, the gasification technology has been tested on several pilot plants. The Gothenburg Biomass Gasification project showed a main achievement with its largest scale of more than 100 MW [30]. The conjunction of biomass gasification with SOFCs is reported to be a promising possibility for electricity and heat cogeneration [28,31]. Being relatively insensitive to microcontaminants, SOFCs can be fed (almost) directly with biogas, upgrading this hydrogen rich fuel to electricity. SOFCs are high temperature devices, making them less suitable for dynamic operation (where quick start-ups are needed) than low temperature fuel cells. However, the elevated temperature favors heat utilization: coupling with a heat engine allows the recovery of thermal energy from the fuel cell exhaust which is converted into additional electricity, resulting in high fuel to end-use efficiencies. This hybridization potential of high temperature fuel cells with gas turbines is even considered to be fostering the development and market penetration of SOFCs [32]. Likewise, thermal coupling of SOFCs with a gasification plant is recommended to achieve higher overall efficiencies (electric and exergetic) [33–35]. Yet very expensive, SOFCs have the potential to extend their market position thanks to their integrability with gasifiers to produce clean electricity from biomass. Biomass Gasification and Solid Oxide Fuel Cell (BGSOFC) are chosen in this study as a projection of potential future biomass-to-electricity conversion technologies.

As efficiency and cost reduction are favored by large-scale adoption, all biomass available was assumed to be used. In other words, the daily bio-waste flow of 1300 ton produced by Amsterdam is transformed in the BGSOFC installation, fostering the effect of energy economy of scale. Besides, possible seasonal variations in organic waste quantity and composition were neglected.

Biomass gasification was mathematically described by a stoichiometric thermodynamic equilibrium model [36,37], returning the volume and heating value of the produced syngas given the organic MSW elemental composition $CH_{1.5}O_{0.59}N_{0.03}$ [38]. Gasification of organic municipal solid waste at 700 °C with an equivalence ratio of 0.2 and a steam to biomass ratio of 0.4 yielded the highest combination of hydrogen production (38.39 dry vol%) and energy efficiency (58.13%). The produced syngas was fed into an efficiency-based SOFC model for further conversion to electricity, with an electrical efficiency of 60% and a fuel utilization factor of 85%. The biomass gasification and SOFC system model can be found in Appendix C.

2.1.3. Load module

The electricity demand (AC loads) was derived from Liander's open-source residential electricity data [39]. The dataset contains average hourly demand for 10,000 inhabitants from 1994–2014 and is scaled to match the total residential electricity demand of Amsterdam in 2014 (792 GWh) [40].

2.2. Optimization methods

The energy system model was used to assess the potential of urban bio-waste in providing flexibility to a sustainably powered Amsterdam. Both enumerative and active-set optimization methods were used to determine the optimal size of the PV and wind installations, while minimizing electricity curtailment.

2.2.1. Enumerative optimization

Enumerative optimization is used as a first step towards finding the optimal combination of all RE resources to meet the electricity demand. The design space of the energy system is defined by a number of decision variables (factors) and their design ranges. Each factor can take on different values (levels) within this design space. Enumeration scans the full design space by sampling the factors in a rectangular grid at predefined levels and simulates the system to find the corresponding response to these levels. In our case-study, the decision variables are the renewable energy coverages κ_{pv} and κ_{wind}, expressed as percentage of the full installed capacity potential. The coverage values were put into the enumeration vector $X_e := [\kappa_{pv}\ \kappa_{wind}]^T$, with possible values between the actual (reference) coverage of both renewable energy technology in Amsterdam and the maximum coverage of 100%. In

other words, the lower boundaries (LB) and upper boundaries (UB) of the decision variables are set to: LB = $[0.045\ 0.38]^T$ and UB = $[1\ 1]^T$. Each element of X_e is discretized into a number of equidistant points within the boundaries defined here-above. In order to keep the amount of variables manageable, no daily variation in bio-waste conversion is considered here. Thus, organic MSW is used directly from the moment it becomes available, with a fixed input of 1300 ton/d.

For each grid point, the total net energy over a year with a daily time-step is calculated, using

$$E_{tot} = \sum_{t=1}^{365} E_{net}(t) \tag{1}$$

where E_{net} is defined as

$$E_{net}(t) = E_{gen}(t) - E_{dem}(t) \tag{2}$$

with E_{dem} the electricity demand and E_{gen} the generated electricity, such that

$$E_{gen}(t) = \frac{E_{pv}(t, \kappa_{pv}) + \frac{E_{wind}(t,\kappa_{wind})}{\eta_{ACDC}} + E_{bio}(t)}{\eta_{DCAC}} \tag{3}$$

Covering the entire design space, enumerative optimization provides an effective tool to visually verify the system's dependencies and to find an approximate minimum of E_{tot} on the domain defined by LB and UB. This minimum is an appropriate starting point with corresponding grid point coordinates (initial guess) for a continuous optimization procedure in a next step.

2.2.2. Active-set optimization

While enumerative optimization provided a first scan of possible RE coverage for a minimal total yearly curtailment, active-set optimization ensures daily energy security, if a feasible solution exists. Besides, active-set optimization provides a more accurate solution, as the solution is not restricted by predefined levels. Coverage of PV and wind are assumed fixed for a year and continuous between LB and UB. The flow of biomass sent into the BGSOFC unit can now vary from day to day in view of minimizing the amount of electricity curtailed. The model was run from July to June, as starting on January 1st would yield an unfeasible solution, as biomass and wind turbines cannot satisfy the large initial winter demand. The starting point is only a problem in the first year the model is run, as stored biomass over the summer contributes to meeting this constraint in later years.

Decision variables for the active-set optimization are defined in Eq. (4). The first 365 elements of this vector are the daily biomass flows going to electricity production F. The last two elements are the PV and wind coverage, in other words the installed capacity expressed as percentage of the maximum potential installed capacity. The size of this active-set vector X_{as} is thus (367x1).

$$X_{as} := \begin{bmatrix} F(1) \\ \vdots \\ F(365) \\ \kappa_{pv} \\ \kappa_{wind} \end{bmatrix} \tag{4}$$

The optimization program is further specified by its objective function J to be minimized, that is

$$\begin{aligned} \underset{X_{as}}{\text{minimize}}\ J &= \sum_{t=1}^{365} E_{gen}(t, X_{as}) - E_{dem}(t) \\ &= \sum_{t=1}^{365} \frac{E_{bio}(t, X_{as}(t)) + E_{pv}(t, X_{as}(366)) + E_{wind}(t, X_{as}(367))}{\eta_{DCAC}} \\ &\quad - E_{dem}(t) \end{aligned} \tag{5}$$

Thus, the program tries to minimize E_{tot} (Eq. (1)) as a function of the decision variables in Eq. (4). However, Eq. (5) is also subject to a set of constraints defining the feasibility domain of the solution. To formulate these constraints, a new variable is introduced: biomass storage S_{bio}. Indeed, when the bio-waste produced is not transformed directly, a storage reservoir is needed to buffer the incoming collected bio-waste before it is sent to the BGSOFC unit. The mass of bio-waste in this reservoir at day t, called $S_{bio}(t)$, is the mass initially stored S_0 plus the sum of organic waste collected F_{in} until day t minus the mass of waste utilized to produce electricity in the BGSOFC unit. F_{in} is assumed constant, while F depends on t

$$S_{bio}(t) = S_0 + \sum_{\tau=1}^{t} F_{in} - \sum_{\tau=1}^{t} F(\tau) \tag{6}$$

Three types of constraints are distinguished: bounds on the decision variables, equality constraints and inequality constraints. The bounds on X_{as} are defined as LB = $[0 \ldots 0\ 0.045\ 0.38]^T$ and UB = $[\infty \ldots \infty\ 1\ 1]^T$. Thus, $F(t)$ can take values between 0 and ∞, while κ_{pv} and κ_{wind} lie between the actual coverage value and a maximum of 1 (100%). No equality constraints needed to be formulated in this problem. However, three static linear inequality constraints IC are defined to bound the solution space:

IC 1 The net daily electricity balance should always be positive or zero:
$E_{net}(t) \geq 0 \qquad for\ t = 1, 2, \ldots, 365$
$E_{net}(t) = E_{gen}(t, X_{as}) - E_{dem}(t)$

IC 2 The reservoir content should always be positive or zero:
$S_{bio}(t) \geq 0 \qquad for\ t = 1, 2, \ldots, 365$
$S_{bio}(t) = S_0 + \sum_{\tau=1}^{t} F_{in} - \sum_{\tau=1}^{t} X_{as}(\tau)$

IC 3 The absolute change in storage between the start and end of the year should be at most one day of bio-waste inflow:
$-1300 \leq S_{bio}(t = 365) - S_0 \leq 1300$

For implementation in MATLAB, the inequalities are written in the form $AX \leq b$, with $X := X_{as}$. Transcribing the IC's to A and b can be found in Appendix D.

2.3. Sensitivity analysis

In order to test the robustness of the optimal solution found from active-set optimization, the base-case scenario is perturbed in a sensitivity analysis. Changes of 20% were made in the efficiency of the SOFC (parameter change) and in the amount of bio-waste throughput (input changes). The effect of these changes is evaluated with respect to the objective function values, after performing a new optimization step with the perturbed parameters and inputs.

To test the robustness of the model to changing climate, "extreme" climatological years within the 1994–2014 weather dataset were identified, using the yearly sum of irradiations and wind speeds. The year 1998 was found to have the least solar resource, 2003 the most. The year 2010 had the least wind and 1994 the most. Table 1.

Years with the most or the least total renewable resources were sought as well: the yearly sums of irradiance and wind speeds were normalized and added, to create a metric to sort them, identifying 2010 as the year with most renewable resources and 1995 with the least (2 scenarios). Finally, wind and solar were studied also individually, by using an extreme year for each individually (4 scenarios) and using the 20 years average for the other resource, for example: to test a decrease in wind only, the lowest wind speed values of 2010 were taken together with the averaged irradiance and temperature values. The installed wind and solar were taken from the baseline scenario, while the biomass input was smoothed for all scenarios, so that an objective comparison could be made, resulting in either curtailment or shortage. The results of these six scenarios are compared to the baseline scenario, in which also the smoothed biomass input was applied.

Table 1
Cumulative solar irradiation and wind speeds to identify extreme years.

	Minimum	Maximum	Base-case scenario
Wind resource	2010: 39 399 m/s	1994: 48 058 m/s	43 684 m/s
Solar resource	1998: 925 480 W/m^2	2003: 1 117 800 W/m^2	1 037 900 W/m^2

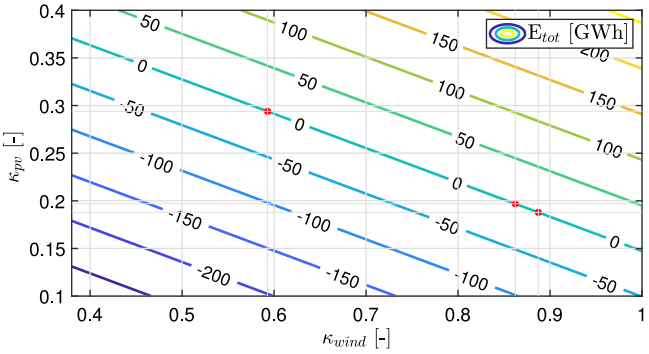

Fig. 2. Enumerative optimization results: Contour representation of E$_{tot}$ over part of the design space (κ_{pv} zoomed in from 0.1 to 0.4 in which the line E$_{tot}$ = 0 falls). The red dots indicate 3 smallest positive E$_{tot}$ values.

3. Results

3.1. Enumerative optimization

Grid enumeration was first performed over the entire design space, before focusing on the region where E_{tot} is zero. 100 equidistant points were taken for κ_{pv} between 0.1 and 0.4 and κ_{wind} between 0.38 and 1. Fig. 2 displays contours of the total energy balance E$_{tot}$ over this selected part. The zero line represents a net even energy balance, where the overall yearly sum of electricity generated equals the electricity demand. Negative E$_{tot}$ indicates an overall shortage of generated energy, which is not a feasible solution. As no direct storage element is defined in the studied islanded system, energy surplus is not stored nor sold to the grid but curtailed. In view of minimizing the curtailment, the optimal RE coverage combination in the design space is found above, close to the net-zero line. The contour lines of E$_{tot}$ confirm the linear relationship between both coverages κ and the total net energy balance and show the sensitivity of E_{tot} with respect to κ_{wind} and κ_{PV}. The three smallest occurrences of E$_{tot}$ are highlighted with a red dot in the figure and correspond to the following wind/PV coordinates: (0.887/0.188), (0.593/0.294), (0.862/0.197). The difference in scales in Fig. 2 indicate that E$_{tot}$ is more sensitive to changes in κ_{PV} than in κ_{wind}. Thus, a change in wind coverage has less impact on E$_{tot}$ than a change in PV as the total coverage capacity differs (175 MW wind for 1100 MW PV capacity).

Formulating the problem in terms of a yearly energy balance does not guarantee day-to-day electricity availability, but focuses on reaching an end-of-the-year break-even. Besides, transforming daily a fixed amount of bio-waste to electricity does not fully comprehend the potential role bio-waste can play in the electricity mix of Amsterdam. In the next section, dynamic modeling is used, with active-set optimization allowing the introduction of a daily positive electricity balance and a changing bio-waste input.

3.2. Active-set optimization

The previously enunciated active-set program is implemented in MATLAB 2019a, with initial guess $X_0 = [1300 \dots 1300 \quad \kappa^*_{PV} \quad \kappa^*_{wind}]^T$. The three 'best' results from enumeration, denoted by κ^*_{PV} and κ^*_{wind}, were taken as starting point for active-set optimization. Initial storage content is taken as S$_0$ = 8.10^4 ton, as a storage buffer was deemed necessary for optimal allocation of biomass over the time-period. Minimizing the amount of surplus electricity produced results in an optimal solution for X_{as}, displayed in Fig. 3. All three initial guesses yielded similar results in terms of coverage values; the one with smallest objective function value was kept. Fig. 3a shows the daily flow of bio-waste collected together with the bio-waste sent to the gasifier/fuel cell for electricity production (from July to July). Fig. 3b displays the amount of biomass stored in the reservoir throughout the year, with a minimum reached in March. The red line in Fig. 3c indicates the daily electricity demand. The yellow, blue and green stacked bars mark the share of PV, wind and bio-energy generated to meet the demand, for a PV and wind coverage of respectively 16.9% and 94.0%. When more energy is generated than needed and thus the colored bars exceed the red line, the surplus electricity is curtailed. Curtailment is explicitly shown in Fig. 3d.

Fig. 3a shows a low $F(t)$ in summer, increasing as winter comes along. Most of the electricity demand is covered by PV panels from April to September (Fig. 3c), in accordance with the inflexible availability of solar energy. From this optimization scenario, 16.9% of the potential PV capacity is needed to cover the loads while keeping curtailment low. This represents a 186 MW installed capacity. Wind turbine installation is being maximized: 165 of the 175 MW potential capacity is used. This derives from the fact that wind turbines deliver most power in the winter, which is in line with the demand pattern. As less bio-waste is used in summer-time for electricity production, the amount of biomass stored increases (Fig. 3b). By mid-September, a maximal storage of 105 kton biomass is reached. Considering a density of received organic waste of 514 kg/m^3, this represents a stored volume of 204,000 m^3][41]. As a comparison, the largest storage tank in the Netherlands situated in the harbor of Rotterdam for oil storage has a capacity of 114,000 m^3 [42]. In fall and winter, the biomass from the reservoir is used in the BGSOFC unit to provide for the electricity demand associated to shorter days and lower temperatures. A maximum $F(t)$ of 3128 tons is reached in mid-December. Electricity is being curtailed in summer, when inflexible generation by PV and wind is most important. Some biomass is still sent to electricity production on days with curtailment, in order to use all bio-waste and refrain from accumulation. Spring and summer can therefore be used for system maintenance, thus reducing curtailment. At the end of the year, 785 MWh of electricity is being curtailed, or 0.1% of the annual electricity demand in Amsterdam.

3.3. Sensitivity analysis

Sensitivity analyses were performed for the active-set optimization, where the SOFC efficiency and the bio-waste throughput were varied.

3.3.1. Total net energy sensitivity to SOFC efficiency

While the gasifier efficiency has been determined extensively based on the input stream of bio-waste (Appendix C), SOFC electrical efficiency of 60% (range from 55% to 65%) was taken directly from literature [43]. Many factors can affect this efficiency, such as gas composition, amount of impurities contained in the gas or age of the fuel cell stack [44]. To test the effect of SOFC efficiency on the total net energy, scenarios were run with SOFC efficiency of 55% and 65% respectively. The results are shown in Table 2.

SOFC efficiency changes affect the outcome of the objective function at the optimal X_{as} $J(X^*)$. A 5% higher efficiency allows to cut down all electricity curtailed. A 5% lower SOFC efficiency leads to a 1.7 times higher overproduction compared to the base-case; the lower electricity

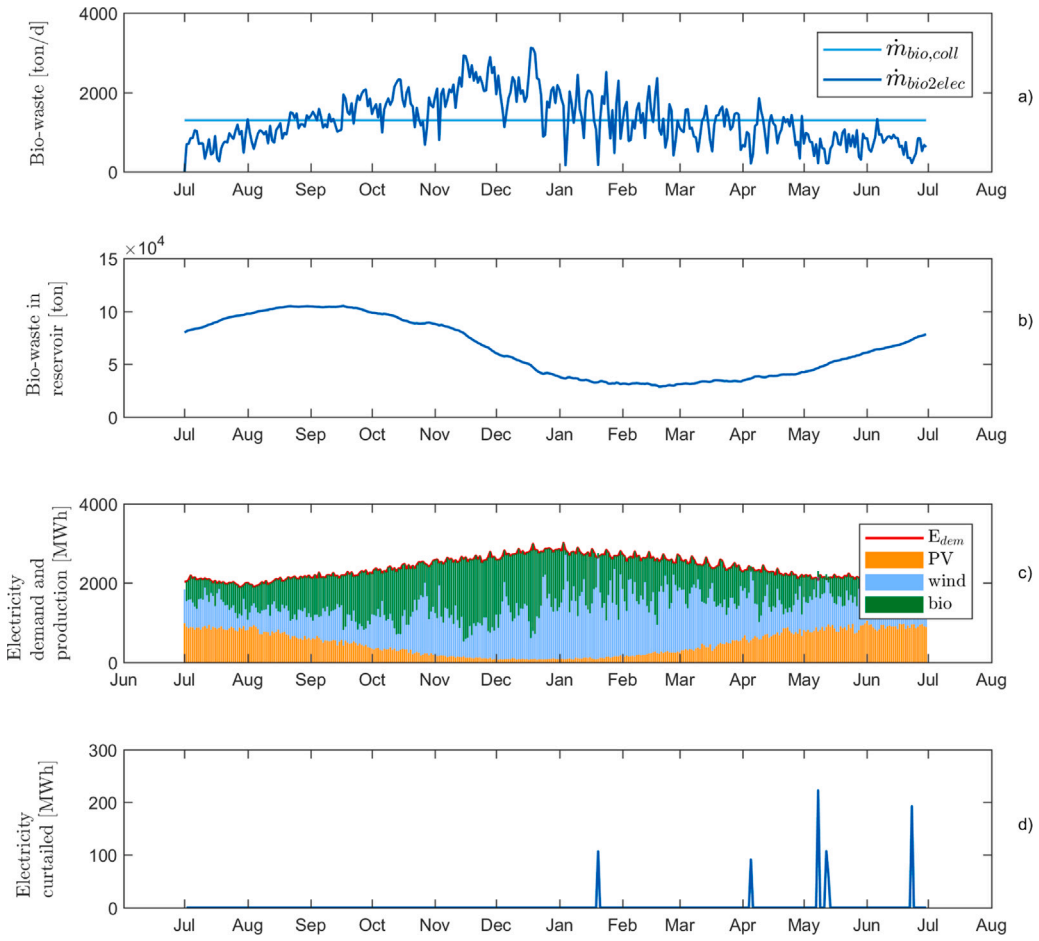

Fig. 3. Active-set optimization results. (a) Daily flowrate of bio-waste collected and bio-waste sent to the BGSOFC unit for electricity generation. (b) Mass of bio-waste stored in reservoir. (c) Electricity demand (red line) and allocation of electricity generation among the different sources (colored bars). (d) Electricity surplus being curtailed. These results are based on $\kappa_{PV} = 0.169$ and $\kappa_{wind} = 0.940$. (For interpretation of the references to color in this figure legend, the reader is referred to the web version of this article.)

Table 2
Outcome of sensitivity analysis with respect to SOFC electrical efficiency.

Run	η_{SOFC} [%]	$J(X^*)$ [MWh]	κ_{PV}	κ_{wind}
Minimal η_{SOFC}	55	1,304	0.224	0.863
Base-case	60	785	0.169	0.940
Maximal η_{SOFC}	65	1e−4	0.148	0.921

production by the SOFC is compensated by a higher coverage in PV. Being both uncontrollable generators, the amount of energy curtailed $J(X^*)$ increases. The overall PV and wind strategy remain relatively similar despite the changes in the SOFC efficiency parameter. A SOFC efficiency of 55% leads to an increased PV coverage from about 16.9 to 22.4%, or 60 MW additional installed capacity and the wind coverage decreases to 86.3% (-14 MW). The net additional RE capacity needed to compensate for the loss in biomass energy is 46 MW. Increasing the SOFC efficiency allows to reduce the PV coverage to 14.8% and the wind coverage to 92.1% (-23 MW and -4 MW resp.), or an overall decrease in RE needed of 27 MW.

To conclude, the total net energy is sensitive to the SOFC efficiency: a lower η_{SOFC} results in increased cost of energy as more electricity is curtailed. This situation will occur as the fuel cell ages: irreversible losses start decreasing the electrochemical device's efficiency. To guarantee renewable electricity supply, policy makers can choose to expand solar coverage, or replace the modules with newer, more efficient ones. Nonetheless, as a controllable source is being replaced by an inflexible one, and more electricity will be wasted. The results of this sensitivity analysis confirm the hypothesis that more biomass usage increases flexibility and thus decreases curtailment.

3.3.2. Total net energy sensitivity to bio-waste throughput

In the model, a daily organic MSW stream of 1300 ton/day was used as bio-waste input. The stream is assumed to be directly and totally available for electricity production. In reality, it is possible that less biomass can be used in the BGSOFC unit, for example as a result of losses between the inhabitants and the electricity production unit. To take into account this uncertainty, a sensitivity analysis was performed to assess the role of changes in the biomass input on the total net energy.

The results of varying the daily available flowrate of biomass ± 20% are displayed in Fig. 4. The assumption that all biomass available is used throughout the year still holds in this sensitivity analysis. The effect of changing the input biomass on the optimal amount of curtailed electricity (black line), together with its associated PV (orange) and wind (blue) coverages, is shown in Fig. 4. As the input biomass decreases, the coverage of PV increases to compensate for the loss in energy production, as well as wind for the -20% case. However, from this slight increase in RE coverage, electricity is produced less flexibly than with higher biomass input, resulting in higher levels of curtailment. In other words, the system appears vulnerable to a decrease in biomass availability. An increase in bio-waste throughput causes a slight decrease in the need for renewables in the form of solar and wind and decreases the curtailment to almost zero, thanks to the controllability of biomass for electricity production. Besides analyzing

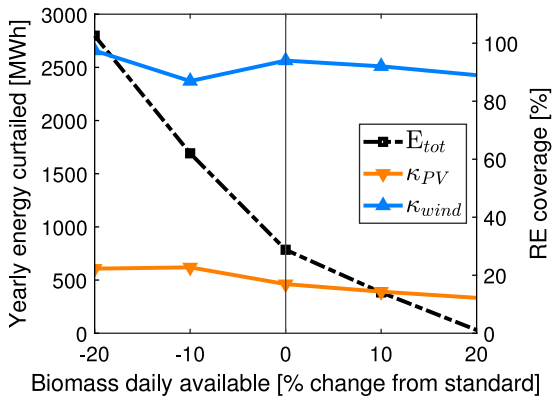

Fig. 4. Effect of changing input bio-waste on total net energy. (For interpretation of the references to color in this figure legend, the reader is referred to the web version of this article.)

the effect of a change in bio-availability, this sensitivity analysis increases the understanding of the modeled system by highlighting the inflexibility of the wind and solar resources and proving the positive role of biomass usage in providing a controllable RE source.

The effect of climate was studied with 6 scenarios in comparison to the baseline. The biomass input was smoothed for the whole year and not matched on an hourly basis, while installed wind (186 MW) and solar (165 MW) were fixed (see Figs. 5 and 6).

Comparing the amount of curtailment and shortage of electricity of this smoothed baseline (with average meteorological data), with the different "extreme weather" scenarios yielded the following results:

- Because of the smoothed biomass input, the baseline had times of electricity shortage and of abundance, resulting in a slight overall excess of electricity of 4 GWh.
- Little renewable resources (2010) resulted in a large amount of shortage and curtailment of electricity (3.3 times the baseline)
- Plenty renewable resources (1995) resulted in an even larger curtailment (5 times the baseline) and decreased shortage (2.4 times the baseline)
- The effect of min/max irradiance on electricity shortage and curtailment was comparable to the baseline scenario (1.1 to 1.6 times). With minimal irradiation and average wind there is an overall net shortage.
- The effect of min/max wind on short/excess electricity are much larger than the baseline (2.5 to 5.5 times)

While in terms of capacity, it is 186 MW for solar against 165 MW for wind. The differences might be explained by the fact that wind speeds count to the power 3 in the equation for wind energy production, while irradiance is linear with solar production.

4. Discussion

Numerous municipalities are looking for ways to become more sustainable and change their energy portfolio accordingly. While covering city roofs with PV panels and installing wind turbines could fulfill their yearly electricity demand, providing sustainable flexibility to match actual demand and supply remains a challenge. In this study, urban bio-waste was used to provide inter-seasonal flexibility to Amsterdam. An active-set optimization program was formulated to assess daily bio-electricity production, PV and wind installed capacities needed to provide daily electricity security to the Dutch capital, while minimizing yearly curtailment. Using 1300 ton bio-waste per day yielded curtailment values of 785 MWh (0.1% of the yearly electricity demand). This value can be lowered to 384 MWh when increasing the daily biomass throughput by 10%, if, for example, waste from outside the city was to be used.

However, in this study, it was implicitly assumed that biomass can be stored until the moment of usage, without alteration in properties. The relative high moisture content of bio-waste material such as fruit and vegetable peels makes it prone to decomposition with formation of fungus and spores. Besides, organic MSW may also contain small animal carcasses, whose long-term storage would lead to putrefaction, releasing a variety of gases: methane, carbon dioxide, hydrogen, ammonia, hydrogen sulfide, and mercaptans [45]. From the results, bio-waste is to be stored at least on a seasonal basis in order to fulfill the winter demand. In fact, some biomass will even be stored on a yearly basis, as a buffer of $8x10^4$ ton was found to be necessary to guarantee minimal curtailment values. In order to avoid an environmental disaster, heating can be used to dry and sterilize the waste, using for example waste heat from the power plant to reduce the biomass moisture content. 155 GWh of heat is available yearly from the SOFC, which is too small to be used for residential district heating purposes (merely 5% of the total needed) but large enough to dry the bio-waste (15 GWh needed). Ideally, a stirrer is needed to dry the biomass evenly, together with a large area to spread the material (corresponding to an impractical 13 hectares at 2m depth) [12].

Instead of storing bio-waste, the syngas from the biomass gasification could be stored and thus avoiding the practical problems of bio-waste storage. For instance, after some technical modifications, the syngas can be stored in branches of the existing gas distribution network, as reduction of natural gas usage in a renewable energy system will give room for storage of other gasses. Given a syngas production from biomass of approximately 1.4 kg or 2.3 m^3 syngas/kg biomass (both wet weights) leads to a re-scaling of Fig. 3b. Moreover, in terms of hydrogen, approximately 43 g H_2/kg biomass, including the water gas shift reaction 54 g H_2/kg biomass and after purification to 99.97% with an efficiency of 67% 36 g H_2/kg biomass, can be recovered through gasification. Consequently, for a maximum bio-waste storage of 105 kton this implies a maximum storage of H_2 of approximately $4.1x10^6$ kg. The other subfigures of Fig. 3, however, will not be affected by this change in storage.

From Fig. 3 it can also be seen that the amount of bio-waste supplied to the BGSOFC unit varies largely from day-to-day. However, both transient and partial loading are known causes of voltage irreversibilities in fuel cells, lowering the life-time of the device [46]. Although load variation is needed to create flexibility in the electricity system, losses can be alleviated by gradually supplying the bio-waste and reducing day-to-day variation. A gradual bio-waste supply will deviate from the solution found in Section 3.2, meaning daily electricity security might not be met anymore, or more electricity might be curtailed.

In fact, allowing small electricity deficits could add new degrees of freedom to the problem. The hard constraint on energy availability was deemed necessary in the energy system model, but probably irrelevant in reality. Many more components will come into play such as storage or (inter)national green energy trading, allowing energy produced at a different time or place to be used, thus moving away from the island mode and finding a trade-off between self-sufficiency at city-level and curtailment. Indeed, electricity production should not be limited to the geographical boundaries of Amsterdam. For example, wind turbines are more profitable when installed outside urban areas to harvest higher wind velocities and preserve the urban living space. Interconnecting energy systems will thus result in a reduction of installed capacity of the renewables and (in general) a reduction of costs.

It should be stressed that the conclusions reached in this study are dependent on assumptions and priorities. For example, sustainability and energy security were chosen as leitmotivs to characterize the model and formulate the optimization problem, in spite of the economic component. In the energy system model with the aim to investigate the potential of urban bio-waste, the use of all bio-waste available in a year is forced upon the system, regardless of the associated costs. In practice,

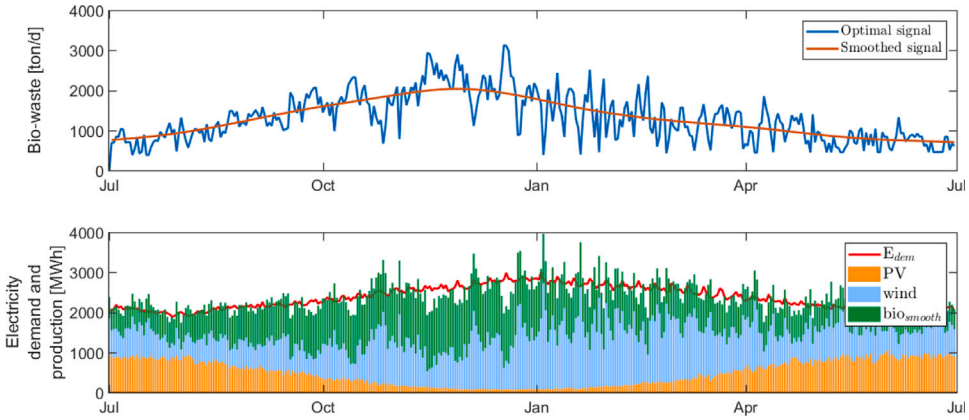

Fig. 5. Smoothed biomass input to study the effect of wind and solar in extreme years.

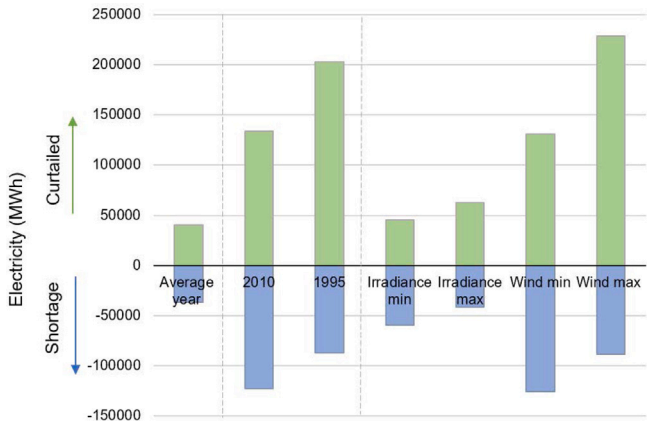

Fig. 6. Effect of weather conditions on curtailment or shortage, using smoothed biomass input.

policy makers will choose an energy system based on its economic competitiveness. In further studies, the costs of each renewable energy technology (PV, wind and bio-waste) could be weighed against its benefits (availability, flexibility), using for example Levelized Cost of Electricity (LCOE) as economic metric. LCOE measures the lifetime costs of a technology (or combination of technologies), divided by its energy production. From literature, the cost of PV and wind systems appear to be relatively low, with a LCOE of 8–10 €cts/kWh for residential roof PV and 4–6 €cts/kWh for onshore wind turbines [47]. Estimates of BGSOFC LCOE reach almost 30 €cts/kWh [48], representing a potential obstacle for the deployment of the technology. Thus, given the BGSOFC LCOE, it is clear that as yet a PV–wind mix is more profitable than the proposed energy mix, at the expense of higher curtailment. Nevertheless, BGSOFC systems are in a much younger stage of development than PV and wind systems, meaning the costs could decrease in the future.

A final consideration is the issue of flexibility at all time scales. Today's flexibility is provided by conventional power plants, regardless of the time-scale. Coal or gas-fired plants are designed with both main units and fast-starting units, to cover base-load and ramping respectively. In an all-renewable scenario, new technologies must be found to guarantee reliable energy supply at all time-scales, as well. Most probably, there will not be a single robust technology able to start and stop many times, with low minimum load levels, little heat losses and quick ramp-up speed. A combination of technologies and techniques will be necessary to replace the conventional carbon-emitting power plants. While batteries are commonly considered as the best option for short-term storage to supply fast transient and ripple power, the results of this study offer possibilities for long-term flexible power generation [3].

Other sources of flexibility are found in literature, which can be combined in the future to ensure reliable electricity supply. Hydrogen-based technologies are rising in popularity, with the possibility of using natural gas pipelines to transport and store hydrogen. Hydrogen can be produced in times of surplus electricity production via electrolysis and be stored for later usage. Studies have also demonstrated how electric fuel cell vehicles can provide fast frequency reserves to a grid, offering new possibilities of short-term flexibility without the need of building new power plants [49–52]. Redox flow batteries have also great advantages to provide flexibility in future energy systems: they can offer high power as well as long duration, are not site-dependent (like Pumped Hydro-Storage) and are expected to perform more than 10,000 cycles without significant aging (against 5000 for Li-ion batteries) [53,54].

Not only technologies on the supply-side can bring flexibility in the energy network, but also tools on the demand-side. Demand-response programs involve pro-active consumers to adapt their energy use behavior, shaving off peaks in demand and using electricity when abundant, affordable and clean [55,56]. In the end, a combination of complementary flexibility providing options will be used in the future.

Future work can expand towards biomass drying and syngas storage after gasification, size and scaling of additional DC storage options, introducing economic, environmental and social factors, green energy trading, integrating demand response measures, and finally practical implementation and corresponding implications at distributed grid level.

5. Conclusion

In the present work, an optimization based framework was built to assess the potential of urban bio-waste as a source of flexible renewable electricity. Amsterdam was taken as an islanded case-study, where electricity is produced locally by photovoltaics, wind turbines and biomass in a biomass gasification/solid oxide fuel cell (BGSOFC) system. Two optimization methods were used to determine the optimal size of each renewable energy installation while minimizing yearly overall electricity curtailment.

Firstly, enumerative optimization provided an initial mapping of the possible combinations for PV and wind turbines, given a fixed daily bio-waste usage. A minimum positive yearly net energy E_{tot} was found for a PV coverage of 18.8% and wind coverage of 88.7%. Secondly, active-set optimization resulted in optimal RES sizing with flexible daily bio-waste usage, not only to guarantee year-round but also day-to-day energy security. This resulted in a PV coverage of 16.9% and a wind coverage of 94.0% (resp. 186 and 165 MW installed capacity). More biomass was used in the winter, when PV panels were unable to provide for the needed energy. Finally, sensitivity analysis demonstrated the

optimal sizing to be robust, showing little variations upon changing SOFC efficiency or biomass inputs.

Bio-waste was demonstrated to hold the potential of bringing seasonal flexibility to future sustainable electricity systems. The methodological framework presented here can help researchers and decision-makers to quickly explore the possibilities of urban bio-waste usage in the electricity mix.

Acknowledgments

We are thankful to the KNMI, Liander and AEB for providing resp. the weather, electricity consumption and bio-waste data of Amsterdam. We would like to express our gratitude to Dr. Kiewidt, Biobased Chemistry and Technology at Wageningen University & Research, for his help on the biomass gasifier model.

Appendix A. Photovoltaic system model

The output power generated by photovoltaics is described in Eq. (A.1), with I_t being the tilted radiation received at the surface of the panel, η_{pv} the panel's efficiency, A_{tot} the total roof area of Amsterdam available for PV (11 km^2, [26]) and κ_{pv} the percentage of this area actually covered by solar panels.

$$P_{pv} = I_t \ \eta_{pv} \ A_{tot} \ \kappa_{pv} \tag{A.1}$$

Photovoltaic power generation first depends on input solar irradiation. The KNMI data used are global irradiation data, thus including the diffuse and direct components of the incoming solar beam. The data are provided as horizontal measurements. However, PV panels are tilted to make solar rays reach their surface perpendicularly, as this maximizes power production. In the Netherlands, a 37 ° tilt and an orientation to the south is assumed to provide maximal sunlight interception [57]. The horizontal irradiation data are corrected using a correcting ratio R_b to calculate the irradiation I_t on panels with optimal tilt.

$$I_t = R_b \ I_{hor} \tag{A.2}$$

$$R_b = \frac{cos(\alpha_i(t))}{cos(\alpha_z(t))} \tag{A.3}$$

α_i is the incidence angle between the beam radiation on the panel and the beam normal to the panel, while α_z is the zenith angle. R_b is calculated for each hour of the day at the latitude and longitude of Amsterdam [57].

The efficiency of a PV panel η_{pv} is highly dependent on the temperature of the solar cell T_{cell}. This meteorological effect can be evaluated using the following simplified thermal model [57]:

$$\eta_{pv} = \eta_{ref} \ \eta_{pc} \ (1 - 3.2 \ 10^{-3} \ |T_{cell} - T_{ref}|) \tag{A.4}$$

where η_{ref} is the reference PV conversion efficiency, taken as 18% for mono-crystalline silicon [26]. A power conditioning efficiency η_{pc} of 95% is assumed, which covers the efficiencies of the maximum power point tracker and the inverter [58]. The temperature inside the PV module is evaluated using an empirical linear relationship between the T_{cell} - T_a and I_t based on the Nominal Operating Cell Temperature (NOCT). NOCT is a reference point temperature of solar cells under 800 W/m^2 irradiance I_{ref}, 20 °C ambient temperature T_{ref} and 1 m/s wind speed. T_{NOCT} is taken as 45 °C [57].

$$T_{cell} = T_a + \frac{T_{NOCT} - T_{ref}}{I_{ref}} \ I_t \tag{A.5}$$

Table B.3
Specifications of the Enercon 3MW wind turbine.

Rated power	3	MW
Hub height	92	m
Rated wind speed	12	m/s
Cut-in wind speed	2	m/s
Cut-out wind speed	25	m/s

Table C.4
Proximate, ultimate and calorific analyses for organic municipal solid waste, wood and sludge [38]. Dry ash free (daf) weight is discerned from as received (ar) weight.

		Org MSW	Wood	Sludge
C	wt.% daf	51.66	50.71	39.43
H	wt.% daf	6.47	6.08	6.33
O	wt.% daf	40.50	42.82	49.03
N	wt.% daf	1.75	0.39	3.89
Moisture content	% ar	35.00	17.00	75.25
Ash content	% dry base	30.30	2.26	24.15
Lower heating value	MJ/kg daf	19.94	18.88	14.14
Lower heating value	MJ/kg ar	9.07	15.32	2.69

Appendix B. Wind turbine system model

Different models to predict wind turbine power production are used in literature depending mainly on the purpose of modeling and available data [59]. In this paper, the wind power output is approximated using a cubic function as follows:

$$P_w(t) = \begin{cases} 0, & v(t) < v_{cut-in} \ or \ v(t) \geq v_{cut-out} \\ P_{rated} \ \frac{v(t)^3 - v_{cut-in}^3}{v_{rated}^3 - v_{cut-in}^3}, & v(t) \geq v_{cut-in} \ \& \ v(t) < v_{rated} \\ P_{rated}, & v(t) \geq v_{rated} \ \& \ v(t) < v_{cut-out} \end{cases} \tag{B.1}$$

with rated power P_{rated}, cut-in windspeed v_{cut-in}, rated windspeed v_{rated} and cut-out windspeed $v_{cut-out}$. Characteristics of the Enercon 3 MW wind turbine are used as parameters, specified in Table B.3 [60].

Wind speed data from the KNMI at Schiphol are used, which were measured at 10 m height. To correct for the vertical differences in wind speeds, the power law described in Eq. (B.2) is used [61]. Power law exponent α is taken as 1/7, which is the empirical coefficient used for onshore wind speed adjustment [61].

$$v_{hub} = v_{10} \ (\frac{h_{hub}}{10})^{\alpha} \tag{B.2}$$

P_w is the AC power produced by a single Enercon 3 MW type of wind turbine. An inverter efficiency of 90% is used to convert the AC power to DC power, in accordance to the system design shown in Fig. 1.

Appendix C. Biomass gasification and SOFC system model

Bio-waste is sent to a gasifier for conversion to syngas, later to be used in a SOFC for production of electricity. Gasification is modeled by a Stoichiometric Thermodynamic Equilibrium Model (STEM). The normalized elemental composition of biomass is used as input to derive the yield and composition of the output synthesis gas (mainly H_2 and CO) [29,36,37]. Bio-waste elemental composition ($CH_{1.5}O_{0.59}N_{0.03}$) is derived from biomass ultimate analysis (Table C.4, [38]). Values for wood and sludge are displayed as a comparison.

The main equation used in the STEM model is the gasification reaction equation (Eq. (C.1)), with each x being the stoichiometric coefficients of the producer gas, n_w are the moles water per mole biomass and x_g are the moles air per mole biomass.

$$\begin{aligned} &CH_{1.5}O_{0.59}N_{0.03} + n_w H_2O + x_g(O_2 + 3.76N_2) \rightarrow \\ &x_1CO + x_2H_2 + x_3CO_2 + x_4H_2O + x_5CH_4 + (0.03/2 + 3.76x_g)N_2 \end{aligned} \tag{C.1}$$

x_g can be determined by setting a fixed Equivalence Ratio actual over stoichiometric air ($ER = x_g/(1 + 0.25a - 0.5b)$) [29]. Besides being

Table C.5
Effect of changing ER and SBR on syngas' hydrogen and water content and on energy efficiency of the process. Feed = organic MSW, Tgas = 700 °C. Steam temperature is warmed up to gasifier temperature.

ER [–]	SBR [–]	H_2 [dry vol%]	H_2O [tot vol%]	η_{EN} [%]
0.2	0	36.33	23.19	48.80
0.3	0	29.58	24.93	55.60
0	1	59.22	44.70	58.52
0	0.4	56.96	31.25	46.38
0.2	1	40.31	44.48	68.55
0.2	0.4	38.39	33.11	58.13

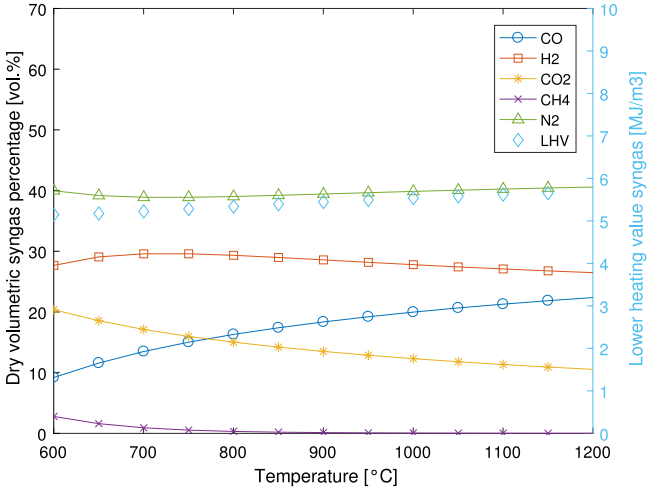

Fig. C.7. Effect of temperature on dry volumetric syngas composition and LHV of organic MSW with air as gasifying agent. ER = 0.3.

determined by the moisture content of the biomass, n_w is also dependent on the Steam to Biomass Ratio (SBR), as steam is often used as a gasifying medium together with oxygen from the air. Stoichiometric coefficients x are obtained by solving 5 equations using Newton–Raphson in the MATLAB 2019a platform: 3 elemental balances (C, H and O), and 2 equilibrium reactions (Water-Gas-Shift and methanation sub-reactions) [37]. From there, the lower heating value of the syngas can be derived using $LHV_{SG} = 10.8\ Vd_{H_2} + 12.6\ Vd_{CO} + 35.9\ Vd_{CH_4}$, where V_d indicates the dry volumetric percentage of syngas [36].

Temperature, ER and SBR of the gasifier were chosen to maximize the final electricity production. First, the STEM was run for temperatures ranging from 600 to 1200 °C, with air as gasifying agent and ER fixed at 0.3 (Fig. C.7). The maximum hydrogen content was reached at a reactor temperature of 700 °C, making 700 °C the default temperature chosen for further computations. In terms of gasifying medium, a trade-off between air and steam gasification had to be found. Air gasification is cheap but yields limited amount of hydrogen gas. The main disadvantage lies in the inert nitrogen brought into the system, which dilutes the syngas produced. A possibility to alleviate this shortcoming is to decrease the equivalence ratio, while keeping in mind that low oxygen levels also lead to low energy efficiencies. Steam gasification comes at a higher downstream processing cost due to the higher water content in the syngas, but allows a more efficient conversion of biomass to syngas [36,62].

Several combinations of ER and SBR are listed in Table C.5, showing the associated hydrogen production, water content of the syngas and energy efficiency. Energy efficiency is defined as $\eta_{EN} = \sum_{prod} H / \sum_{reac} H$, with H the total enthalpy of resp. the reactants and products [37,63,64]. Combining a low ER (0.2) and a low SBR (0.4) yields a satisfactory energy efficiency of 58.13%, a low water content (33.11%) together with a reasonable hydrogen production (38.39%), and are chosen as operating parameter in the gasifier model.

Power production in the solid oxide fuel cell stack is described as follows:

$$P_{SOFC} = \frac{LHV_{SG}\ V_d tot\ \eta_{SOFC}\ U_f\ \eta_{DCDC}}{3600} \tag{C.2}$$

$V_d tot$ is the total dry volume of syngas produced. The electrical efficiency of the solid oxide fuel cell η_{SOFC} is taken as 60% [43], the fuel utilization U_f as 0.85 [29] and the converter efficiency η_{DCDC} as 90%.

Appendix D. Formulation of inequality constraints in the form of $AX \leq b$

IC 1 The net daily electricity balance should always be positive or zero:

$$E_{gen} - E_{dem} \geq 0 \qquad for\ t = 1, 2, \ldots, 365$$
$$E_{dem} - E_{gen} \leq 0$$

where E_{gen} is a linear function of X such that $E_{gen}(t) - E_{dem}(t)$ can be written as $A_1 X \leq b_1$, using the 'equationsToMatrix' function in Matlab.

$$A_1 = \begin{bmatrix} a_1 & 0 & \cdots & 0 & b_1 & c_1 \\ 0 & a_2 & \cdots & 0 & b_2 & c_2 \\ \vdots & \vdots & \ddots & \vdots & \vdots & \vdots \\ 0 & 0 & \cdots & a_{365} & b_{365} & c_{365} \end{bmatrix} \qquad b_1 = \begin{bmatrix} d_1 \\ d_2 \\ \vdots \\ d_{365} \end{bmatrix}$$

IC 2 The reservoir content should always be positive or zero:

$$S_{bio}(t) \geq 0 \qquad for\ t = 1, 2, \ldots, 365$$
$$\text{with } S_{bio}(t) = S_0 + \sum_{\tau=1}^{t} F_{in} - \sum_{\tau=1}^{t} F(\tau)$$
$$\text{such that } S_0 + \sum_{\tau=1}^{t} F_{in} - \sum_{\tau=1}^{t} F(\tau) \geq 0$$
$$-\sum_{\tau=1}^{t} F(\tau) \geq -S_0 - \sum_{\tau=1}^{t} F_{in}$$
$$\sum_{\tau=1}^{t} F(\tau) \leq S_0 + \sum_{\tau=1}^{t} F_{in}$$

Given $F_{in} = 1300$,

$$A_2 = \begin{bmatrix} 1 & 0 & 0 & \cdots & 0 \\ 1 & 1 & 0 & \cdots & 0 \\ 1 & 1 & 1 & \cdots & 0 \\ \vdots & \vdots & \vdots & \ddots & \vdots \\ 1 & 1 & 1 & \cdots & 1 \end{bmatrix} \qquad b_2 = \begin{bmatrix} S_0 + 1300 \\ S_0 + 2 * 1300 \\ S_0 + 3 * 1300 \\ \vdots \\ S_0 + 365 * 1300 \end{bmatrix}$$

IC 3 The change in storage between the start and end of the year should be at most one day of bio-waste inflow
$-1300 \leq S_{bio}(t = 365) - S_0 \leq 1300$
The two parts are separated for the calculation.

IC 3a $-1300 \leq S_{bio}(t = 365) - S_0$:

$$-1300 \leq S_{bio}(t = 365) - S_0$$
$$-1300 \leq S_0 + \sum_{\tau=1}^{365} F_{in} - \sum_{\tau=1}^{365} F(\tau) - S_0$$
$$\sum_{\tau=1}^{365} F(\tau) \leq 1300 + \sum_{\tau=1}^{365} F_{in}$$
$$\sum_{\tau=1}^{365} F(\tau) \leq 366 * 1300$$

$$A_{3a} = \begin{bmatrix} 1 & 1 & \cdots & 1 & 0 & 0 \end{bmatrix} \qquad b_{3a} = 366 * 1300$$

IC 3b $S_{bio}(t = 365) - S_0 \leq 1300$:

$$S_{bio}(t = 365) - S_0 \leq 1300$$

$$S_0 + \sum_{\tau=1}^{365} F_{in} - \sum_{\tau=1}^{365} F(\tau) - S_0 \leq 1300$$

$$-\sum_{\tau=1}^{365} F(\tau) \leq 1300 - \sum_{\tau=1}^{365} F_{in}$$

$$-\sum_{\tau=1}^{365} F(\tau) \leq -364 * 1300$$

$$A_{3b} = \begin{bmatrix} -1 & -1 & \cdots & -1 & 0 & 0 \end{bmatrix} \qquad b_{3b} = -364 * 1300$$

References

[1] United Nations, Adoption of the Paris agreement, Framework convention on climate change, 2015.

[2] European Parliament, Directive on the promotion of the use of energy from renewable sources, Directive (EU) 2018/2001 - PE/48/2018/REV/1, 2018.

[3] H. Holttinen, A. Tuohy, M. Milligan, E. Lannoye, V. Silva, S. Müller, L. Sö, et al., The flexibility workout: managing variable resources and assessing the need for power system modification, IEEE Power Energy Mag 11 (6) (2013) 53–62.

[4] P. Chiradeja, Benefit of distributed generation: A line loss reduction analysis, in: Transmission and Distribution Conference and Exhibition: Asia and Pacific, IEEE, 2005, pp. 1–5.

[5] Y. Yoldaş, A. Önen, S. Muyeen, A.V. Vasilakos, İ. Alan, Enhancing smart grid with microgrids: Challenges and opportunities, Renew. Sustain. Energy Rev. 72 (2017) 205–214.

[6] H. Yang, W. Zhou, L. Lu, Z. Fang, Optimal sizing method for stand-alone hybrid solar–wind system with LPSP technology by using genetic algorithm, Sol. Energy 82 (4) (2008) 354–367.

[7] X. Luo, J. Wang, M. Dooner, J. Clarke, Overview of current development in electrical energy storage technologies and the application potential in power system operation, Appl. Energy 137 (2015) 511–536.

[8] D. Azari, S.S. Torbaghan, H. Cappon, K.J. Keesman, H. Rijnaarts, M. Gibescu, Exploring the impact of data uncertainty on the performance of a demand response program, Sustain. Energy Grids Netw. 20 (2019) 100262.

[9] X. Wang, A. Palazoglu, N.H. El-Farra, Operational optimization and demand response of hybrid renewable energy systems, Appl. Energy 143 (2015) 324–335.

[10] Eurostat, Energy statistics - supply, transformation and consumption, 2016, https://ec.europa.eu/eurostat/cache/metadata/en/nrg_10_esms.htm. (Accessed 25 July 2019).

[11] Dutch Ministry of Economic Affairs (Ministerie van Economische Zaken), Biomass 2030: Strategic Vision for the Use of Biomass on the Road to 2030, Publication nr 89293, 2015.

[12] A.A. Rentizelas, A.J. Tolis, I.P. Tatsiopoulos, Logistics issues of biomass: The storage problem and the multi-biomass supply chain, Renew. Sustain. Energy Rev. 13 (4) (2009) 887–894.

[13] D. Klass, Biomass for Renewable Energy, Fuels, and Chemicals, Academic Press, London, 1998.

[14] C. Field, J. Campbell, D. Lobell, Biomass energy: the scale of the potential resource, Trends Ecol. Evol. 23 (2) (2016) 65–72.

[15] H.M. Junginger, T. Mai-Moulin, V. Daioglou, U. Fritsche, R. Guisson, C. Hennig, D. Thrän, J. Heinimö, J.R. Hess, P. Lamers, et al., The future of biomass and bioenergy deployment and trade: a synthesis of 15 years IEA Bioenergy Task 40 on sustainable bioenergy trade, Biofuels, Bioprod. Biorefin. 13 (2) (2019) 247–266.

[16] H. Belmili, S. Boulouma, B. Boualem, A. Fayçal, Optimized control and sizing of standalone PV-wind energy conversion system, Energy Procedia 107 (2017) 76–84.

[17] M.D. Al-Falahi, S. Jayasinghe, H. Enshaei, A review on recent size optimization methodologies for standalone solar and wind hybrid renewable energy system, Energy Convers. Manage. 143 (2017) 252–274.

[18] S. Sinha, S. Chandel, Review of recent trends in optimization techniques for solar photovoltaic–wind based hybrid energy systems, Renew. Sustain. Energy Rev. 50 (2015) 755–769.

[19] M.W. Rosegrant, S. Msangi, Consensus and contention in the food-versus-fuel debate, Ann. Rev. Environ. Resour. 39 (2014).

[20] D. Tilman, R. Socolow, J.A. Foley, J. Hill, E. Larson, L. Lynd, S. Pacala, J. Reilly, T. Searchinger, C. Somerville, et al., Beneficial biofuels—the food, energy, and environment trilemma, Science 325 (5938) (2009) 270–271.

[21] P. Balamurugan, S. Ashok, T. Jose, Optimal operation of biomass/wind/PV hybrid energy system for rural areas, Int. J. Green Energy 6 (1) (2009) 104–116.

[22] H. Garrido, V. Vendeirinho, M. Brito, Feasibility of KUDURA hybrid generation system in mozambique: Sensitivity study of the small-scale PV-biomass and PV-diesel power generation hybrid system, Renew. Energy 92 (2016) 47–57.

[23] Dutch National Government (Rijksoverheid), National Action Plan for Energy from Renewable Sources, Directive 2009/28/EG, 2009.

[24] Y. Jiang, E. van der Werf, E.C. van Ierland, K.J. Keesman, The potential role of waste biomass in the future urban electricity system, Biomass Bioenergy 107 (2017) 182–190.

[25] KNMI, Hourly weather data in the netherlands, 2019, https://projects.knmi.nl/klimatologie/uurgegevens/selectie.cgi. (Accessed 23 March 2019).

[26] A. de Buck, J.H. Benner, H.J. Croezen, C. Leguijt, D. Nelissen, Sustainable energy in Amsterdam: opportunities at the horizon, CE Delft, 2009.

[27] J. Kurschner, M. Berkhout, Concept RES: Het bod van deelregio Amsterdam, 2020, https://www.amsterdam.nl/bestuur-organisatie/volg-beleid/coalitieakkoord-uitvoeringsagenda/gezonde-duurzame-stad/klimaatneutraal/regionale-energiestrategie-duurzame/. (Accessed 11 August 2020).

[28] C. Athanasiou, F. Coutelieris, E. Vakouftsi, V. Skoulou, E. Antonakou, G. Marnellos, A. Zabaniotou, From biomass to electricity through integrated gasification/SOFC system-optimization and energy balance, Int. J. Hydrogen Energy 32 (3) (2007) 337–342.

[29] J. Jia, A. Abudula, L. Wei, B. Sun, Y. Shi, Thermodynamic modeling of an integrated biomass gasification and solid oxide fuel cell system, Renew. Energy 81 (2015) 400–410.

[30] A. Alamia, A. Larsson, C. Breitholtz, H. Thunman, Performance of large-scale biomass gasifiers in a biorefinery, a state-of-the-art reference, Int. J. Energy Res. 41 (14) (2017) 2001–2019.

[31] C.O. Colpan, F. Hamdullahpur, I. Dincer, Solid oxide fuel cell and biomass gasification systems for better efficiency and environmental impact, in: Eighteenth World Hydrogen Energy Conference WHEC, 16–21, 2010.

[32] M.A. Azizi, J. Brouwer, Progress in solid oxide fuel cell-gas turbine hybrid power systems: System design and analysis, transient operation, controls and optimization, Appl. Energy 215 (2018) 237–289.

[33] V. Subotić, A. Baldinelli, L. Barelli, R. Scharler, G. Pongratz, C. Hochenauer, A. Anca-Couce, Applicability of the SOFC technology for coupling with biomass-gasifier systems: Short-and long-term experimental study on SOFC performance and degradation behaviour, Appl. Energy 256 (2019) 113904.

[34] L. Fryda, K.D. Panopoulos, E. Kakaras, Integrated CHP with autothermal biomass gasification and SOFC–MGT, Energy Convers. Manage. 49 (2) (2008) 281–290.

[35] C. Bang-Møller, M. Rokni, B. Elmegaard, Exergy analysis and optimization of a biomass gasification, solid oxide fuel cell and micro gas turbine hybrid system, Energy 36 (8) (2011) 4740–4752.

[36] J. George, P. Arun, C. Muraleedharan, Stoichiometric equilibrium model based assessment of hydrogen generation through biomass gasification, Proc. Technol. 25 (2016) 982–989.

[37] A. Bhavanam, R. Sastry, Modelling of Solid Waste Gasification Process for Synthesis Gas Production, NISCAIR-CSIR, India, 2013.

[38] ECN/TNO, Phyllis2: database for biomass and waste, 2019, https://phyllis.nl/Browse/Standard/ECN-Phyllis. (Accessed 14 March 2019).

[39] Liander, Available data, daily profiles, 2014, https://www.liander.nl/partners/datadiensten/open-data/data. (Accessed 22 March 2019).

[40] Municipality of Amsterdam, Amsterdam in Numbers 2015, Research, Information and Statistics (OIS in Dutch), 2015.

[41] Environmental Protection Agency Victoria, Waste materials densities data, 2018, https://www.epa.vic.gov.au/business-and-industry/lower-your-impact/~/media/Files/bus/EREP/docs/wastematerials-densities-data.pdf. (Accessed 2019-07-08).

[42] Wikipedia Energy Agency, Oil tank, 2016, https://nl.wikipedia.org/wiki/Olietank. (Accessed 09-07-2019).

[43] Z.U. Din, Z. Zainal, Biomass integrated gasification–SOFC systems: Technology overview, Renew. Sustain. Energy Rev. 53 (2016) 1356–1376.

[44] P.V. Aravind, M. Liu, High Efficiency Energy Systems with Biomass Gasifiers and Solid Oxide Fuel Cells, Wiley, 2004, pp. 505–524, (Chapter 16).

[45] J. Brooks, Postmortem changes in animal carcasses and estimation of the postmortem interval, Vet. Pathol. 53 (5) (2016) 929–940.

[46] J. Larminie, A. Dicks, M.S. McDonald, Fuel Cell Systems Explained, vol. 2, J. Wiley Chichester, UK, 2003.

[47] Fraunhofer Institute, Levelized Cost of Electricity: Renewable Energy Technologies, Freiburg, Fraunhofer Institute for Solar Energy Systems, 2018.

[48] W. Doherty, Modelling of Biomass Gasification Integrated with a Solid Oxide Fuel Cell System, Dublin Institute of Technology, 2014.

[49] M. Poorte, Technical and Economic Feasibility Assessment of a Car Park as Power Plant Offering Frequency Reserves, TU Delft repository, 2017.

[50] A.J. Van Wijk, L. Verhoef, Our Car As Power Plant, ioS Press, 2014.

[51] C.B. Robledo, L.B. van Leeuwen, A.J. van Wijk, Hydrogen fuel cell scooter with plug-out features for combined transport and residential power generation, Int. J. Hydrog. Energy (2019).

[52] A. Haque, A. Saif, P. Nguyen, S. Torbaghan, Exploration of dispatch model integrating wind generators and electric vehicles, Appl. Energy 183 (2016) 1441–1451.

[53] H. Zhang, X. Li, J. Zhang, Redox Flow Batteries: Fundamentals and Applications, CRC Press, 2017.

[54] M. Uhrig, S. Koenig, M.R. Suriyah, T. Leibfried, Lithium-based vs. vanadium redox flow batteries–a comparison for home storage systems, Energy Procedia 99 (2016) 35–43.

[55] D. Azari, S.S. Torbaghan, H. Cappon, M. Gibescu, K.J. Keesman, H. Rijnaarts, Assessing the flexibility potential of the residential load in smart electricity grids — A data-driven approach, in: 14th International Conference on the European Energy Market (EEM), IEEE, 2017, pp. 1–6.

[56] S. Torbaghan, N. Blaauwbroek, D. Kuiken, M. Gibescu, M. Hajighasemi, P. Nguyen, G. Smit, M. Roggenkamp, H.J., A market-based framework for demand side flexibility scheduling and dispatching, Sustain. Energy Grids Netw. 14 (2018) 47–61.

[57] O. Isabella, A. Smets, K. Jäger, M. Zeman, R. van Swaaij, Solar Energy: The Physics and Engineering of Photovoltaic Conversion, Technologies and Systems, UIT Cambridge Limited, 2016.

[58] S. Diaf, G. Notton, M. Belhamel, M. Haddadi, A. Louche, Design and techno-economical optimization for hybrid PV/wind system under various meteorological conditions, Appl. Energy 85 (10) (2008) 968–987.

[59] V. Sohoni, S. Gupta, R. Nema, A critical review on wind turbine power curve modelling techniques and their applications in wind based energy systems, J. Energy (2016).

[60] Wind turbine models, Enercon E115 3MW, 2019, https://en.wind-turbine-models.com/turbines/832-enercon-e-115-3.000. (Accessed 20 March 2019).

[61] O. Nadjemi, T. Nacer, A. Hamidat, H. Salhi, Optimal hybrid PV/wind energy system sizing: Application of cuckoo search algorithm for Algerian dairy farms, Renew. Sustain. Energy Rev. 70 (2017) 1352–1365.

[62] P. Basu, Gasification theory and modeling of gasifiers, in: P. Basu (Ed.), Biomass Gasification and Pyrolysis, Academic Press, Boston, ISBN: 978-0-12-374988-8, 2010, pp. 117–165, (Chapter 5). http://dx.doi.org/10.1016/B978-0-12-374988-8.00005-2. URL http://www.sciencedirect.com/science/article/pii/B9780123749888000052.

[63] R.M. Felder, R.W. Rousseau, L.G. Bullard, Elementary Principles of Chemical Processes, Wiley NY etc., 1986.

[64] National Institute of Standards and Technology, Chemistry WebBook, 2018, https://webbook.nist.gov/chemistry/. (Accessed 10 May 2019).